# APPLICATIONS OF BIOCONJUGATES AND PEPTIDES FOR THE DEVELOPMENT OF BIOSENSORS

by

Sean Rodich

Submitted in partial fulfillment of the requirements for
Departmental Honors in the Department of Chemistry
Texas Christian University
Fort Worth, Texas

May 4th, 2015

# APPLICATIONS OF BIOCONJUGATES AND PEPTIDES FOR THE DEVELOPMENT OF BIOSENSORS

Project Approved:

Kayla N. Green, Ph. D.
Department of Chemistry
(Supervising Professor)

Michael Chumley, Ph. D.
Department of Biology

Giridhar Akkaraju, Ph. D.
Department of Biology

# ABSTRACT

In an age of technology and precision, it is becoming increasingly important to be able to not just diagnose patients with certain diseases but to quantify their level of illness to allow for an appropriate yet calculated response. One such method of quantifying a person's health is to measure the concentration of a given compound of interest – foreign or not – in the blood or other bodily fluid and use that information to gain insight into the disease/condition's progress at that time. Biosensors are compounds whose high levels of specificity and detectability can allow one to measure the concentration of a given analyte under the proper conditions. As a result, well-designed biosensors have the potential to play a key role in the medical diagnosis of a wide variety of diseases.

As a means to developing ferrocene based biosensors, Hunter Scarborough and coworkers in the Green Research Group synthesized and electrochemically evaluated a library of avidin-sensitive ferrocene-biotin bioconjugates. In an effort to continue these studies, we have reproduced some of the electrochemical studies performed on one such bioconjugate, compound **5**, in a more biologically-relevant environment. Our studies have shown that **5** remains sensitive to the target of interest (avidin) when avidin concentrations are brought as low as 1.875 μM and reactive impurities such as albumin are added to the solution.

In addition, separate experiments were performed on the Aβ-derived peptide KLVFF in an effort to validate the affinity of this peptide for Aβ plaques. While multiple tissue stains were performed to achieve this goal, inconclusive results were insufficient to verify any specificity of KLVFF for Aβ. The next phase of this project is

to continue exploring the relationship between peptide moieties such as KLVFF and Aβ plaques through the use of different antibodies and/or stain techniques. If a relationship between KLVFF and Aβ can be established through these methods, it can be applied to the electrochemical methods utilized with **5** and avidin by attaching the electrochemical moiety of **5** to KLVFF and performing similar electrochemical experiments as done previously in the avidin studies on solutions containing this new bioconjugate and Aβ.

# ACKNOWLEDGEMENTS

I acknowledge Dr. Kayla Green, Hunter Scarborough, and the rest of the Green Research Group. Their insight and expertise have been invaluable to me throughout the research process, and I am confident that I would not be the scientist nor student I am today without their guidance and support. I also acknowledge the teaching faculty of the biology and chemistry departments who have given me the fundamental knowledge I have needed to be successful in the laboratory. I also acknowledge the financial support provided by the Robert A. Welch Foundation (P-1760), TCU RCAF, and TCU INFOR funding sources.

# TABLE OF CONTENTS

# LIST OF FIGURES

# LIST OF TABLES

# INTRODUCTION

In an age of technology and precision, it is becoming increasingly important to be able to not only diagnose patients with certain diseases but also quantify their level of illness to allow for an appropriate, yet calculated response. One such method of quantifying a person's health is to measure the concentration of a given product of disease in the blood or other bodily fluid and use that information to gain insight into the disease/condition's progress at that time. Biosensors are systems that have high levels of specificity and low detection limits that can allow one to measure the concentration of a given analyte under the proper conditions (*1*). As a result, strategically designed biosensors have the potential to play a key role in the medical diagnosis of a wide variety of diseases. The work discussed in this thesis will focus on the development of two separate strategies for the detection of biologically relevant molecules. First, electrochemical biosensors will be presented, followed by the design and synthesis of fluorescent markers for peptides associated with disease.

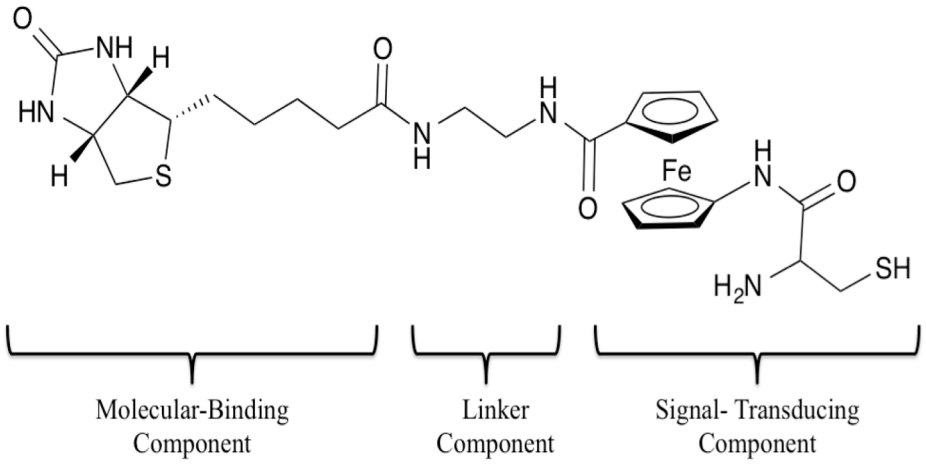


**Figure 1**: Anatomy of an Electrochemical Biosensor

While biosensors are often tuned to be responsive for a given compound or group of compounds, many often follow a similar structural design. In general, a biosensor has three major components: a molecular-binding component, a linker, and a signal-transducing component (*2, 3, 5*). The molecular-binding component is responsible for interacting directly and specifically with the target compound. Since the target compounds are often found in biological systems, the binding components of many biosensors are the same or similar to naturally occurring receptors known to interact with the target compounds in the same biological systems. As a result, biosensors containing these biologically relevant components are often also referred to as bioconjugates (*4, 5*). Upon interaction with the target compound, the molecular-binding component will undergo a change responsible for affecting the entire biosensor's chemical structure or behavior. This change will be carried along the linker component to the signal-transducing component, whose chemical change is often coupled with a change in bioluminescent (*6, 7*), thermal (*8*), or electrochemical energy (*2, 3*). If this change can be detected and quantified by another piece of equipment, the concentration of the original target compound can effectively be measured. In this study, changes in electrochemical signals and redox activity will be used to quantify avidin concentration in solution. The work discussed herein focuses on electrochemical biosensors.

While changes in redox activity can serve as an effective electrochemical signal, most bioconjugates are not intrinsically redox active. The necessary electrochemical measurements, therefore, cannot be made without the introduction of a redox tag. Small inorganic compounds such as ferrocene can serve as effective

tags because of their predictable, well-studied, reversible behaviors in solution (*9-17*). However, a major challenge of utilizing ferrocene is the difficulty of asymmetrically disubstituting ferrocene reliably and efficiently (*17*). Prior studies in our group and others have shown that this can be accomplished through the use of solid phase peptide synthesis and Fmoc-protected terminal amines (*18, 19*). All syntheses described in the next section utilize this solid phase scheme and detail the mechanisms at work.

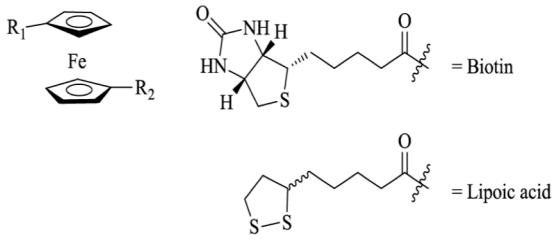


**(1)** $R_1$ = C(=O)NH-$(CH_2)_2$-NH-Biotin; $R_2$ = H
**(2)** $R_1$ = C(=O)NH-$(CH_2)_2$-NH-Biotin; $R_2$ = $NH_2$
**(3)** $R_1$ = C(=O)-Lys-NH-Biotin; $R_2$ = H
**(4)** $R_1$ = C(=O)-Lys-NH(biotinyl-*e*- aminocaproyl); $R_2$ = H
**(5)** $R_1$ = C(=O)NH-$(CH_2)_2$-NH-Biotin; $R_2$ = NH-Cys
**(6)** $R_1$ = C(=O)NH-$(CH_2)_2$-NH-Biotin; $R_2$ = NH-Lipoic acid

**Figure 2**: Library of Ferrocene Bioconjugates (*19*)

Hunter Scarborough and coworkers in the Green Research Group have synthesized a library of ferrocene-containing bioconjugates (compounds **1**-**6**) shown in Figure 2 specific for a target compound: eggwhite avidin. Each compound featured asymmetrically disubstituted ferrocene and was evaluated in solution using cyclic and square wave voltammetry experiments to quantify changes in redox activity observed to occur with changes in avidin concentration. These electrochemical experiments revealed an intense, inversely proportional relationship between avidin concentration and the measured current; as the avidin

concentration was systematically increased from 15-75 μM, both the anodic and cathodic peak currents ($I_{pa}$ and $I_{pc}$, respectively) decreased in a very linear fashion ($R^2$=0.9792). This data suggests that the bioconjugate model for eggwhite avidin developed by Scarborough et al. is valid and practical under the experimental conditions used for measuring avidin concentration in solution through electrochemical analysis (*19*).

My role in this project was to determine the sensitivity and specificity of compound **5**, the biosensor responsible for the strongest signal transmission in the previous experiments, in the presence of both avidin and naturally-occurring blood proteins, namely albumin. Albumin is the most abundant protein in the blood, with an average concentration of approximately 0.66 mM (*20*). As a result, it was important to evaluate whether or not **5** can measure the concentrations of target while in the presence of other biomolecules that are far less prevalent. Additionally, albumin has been shown to be able to react with several different types of compounds (*21*), so it is important to determine if our bioconjugate sensor systems can interact with albumin and, if so, if this interaction is more or less favorable than that with avidin. If the bioconjugate sensor molecules can remain sensitive to avidin while in presence of a comparably abundant and naturally present compound like albumin, the biosensing model developed in the previous experiments is more likely to be viable in a clinical setting.

The sensitivity of compound **5** was evaluated two-fold. First, cyclic and square wave voltammetry experiments were performed on solutions containing **5**, 0.66 mM bovine serum albumin, and 1.875-15 μM eggwhite avidin. These

electrochemical experiments were used to determine whether or not the same inversely proportional trend between avidin concentration and peak currents were observed under these new conditions. Second, molecular modeling using AutoDock Vina was used to both visualize the theoretical interactions between **5** and avidin/albumin and evaluate these interactions from a thermodynamic perspective. The docking results were then used to complement and explain the findings of the electrochemical experiments.

My second project focused on the development of fluorescent markers for peptides associated with Alzheimer's Disease. Alzheimer's Disease (AD) is one of the most serious and common neurodegenerative diseases known today. While its exact causes are still unknown, many studies have shown that the aggregation of amyloid-β (Aβ) monomers and dimers into plaques in the brain is associated with the disease (*22-25*). Further research into Aβ has suggested that, while it primarily aggregates in the brain, it can also be found circulating in the blood and/or cerebrospinal fluid (CSF) of Alzheimer's patients (*26*). Thus, if Aβ concentrations can be measured from blood/CSF samples taken from patients, the results could potentially give insight into not just whether or not a patient has AD but also how far the disease has progressed. A possible extension of the project discussed earlier could involve the development and analysis of an electrically-sensitive bioconjugate with high affinity for Aβ. Numerous studies have shown that the peptide KLVFF can interact specifically with Aβ monomers and plaques (*27-34*), so it is possible that this peptide could serve as the molecular binding component of an Aβ-specific bioconjugate such as C-Fc-KLVFF (shown in Figure 3). The compound could be used

to measure Aβ concentrations using changes in redox activities detected by cyclic and square wave voltammetries, as in the previous studies with avidin.

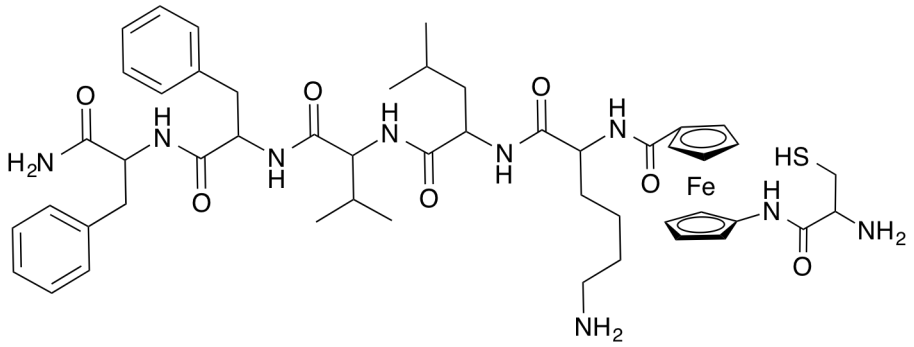


**Figure 3**: C-Fc-KLVFF

However, before such a project could be performed, it would be important to verify that the molecular-binding component of the proposed bioconjugate, KLVFF, could reliably interact with the Aβ plaques. While the electrochemical studies are the end goal of this work, my second project focuses on evaluating the interaction between KLVFF and Aβ plaques in mouse brain tissue. Lab techniques can be used to genetically engineer mice that produce Aβ monomers at an early age, allowing for plaque aggregation within as soon as 2 months of age (*35*). These brain tissues can be collected postmortem and analyzed using a series of staining techniques specific for Aβ. If the stains used have one emission wavelength and the fluorophors attached to KLVFF have another, both the Aβ plaques and the KLVFF will be visible simultaneously if the tissues are exposed to the necessary activation wavelengths and the images captured at each of these wavelengths are overlayed. For example, cyanine 3 (Cy3) has an activation wavelength of 550 nm and an emission wavelength of 570 nm (*36*), and the small molecule fluorescein isothiocyanate has

an activation wavelength of 494 nm and an emission wavelength of 518 nm (*37*). If fluorescein isothiocyanate is attached to the KLVFF molecules exposed to the Cy3-stained tissue samples, both will fluoresce different colors when exposed to 494 nm light and 550 nm light, respectively. Overlaying the images captured at these two wavelengths would allow any interaction between the KLVFF and Aβ to be visualized. The goal of my second project is to use this staining method to verify the KLVFF-Aβ interaction discussed in the literature, as such evidence would allow us to perform the electrochemical studies discussed earlier with confidence.

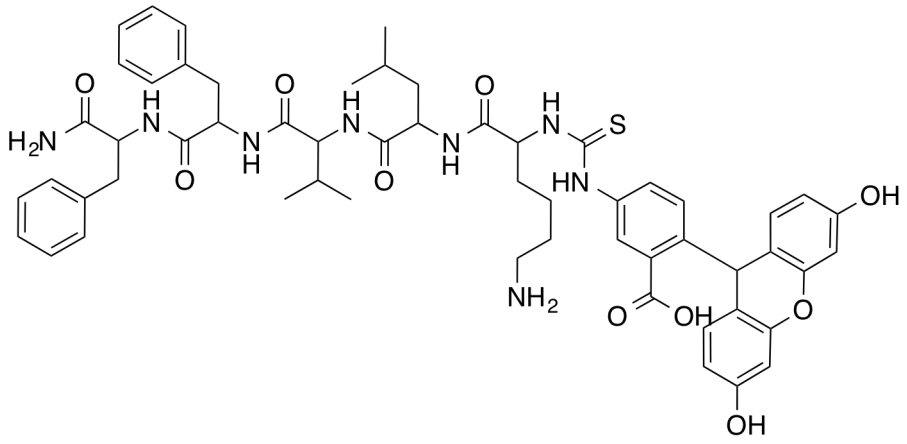


**Figure 4**: KLVFF-Fluorescein Isothiocyanate, Compound **7**

# MATERIALS AND METHODS

## General Procedures

Standard Merrifield techniques were employed for all bioconjugate syntheses using plastic-fritted syringes (10 mL) as reaction vessels to facilitate the multiple additions and removal of reagents and wash solvents. An automated shaker was employed to gently mix the solid phase and reagents. The ninhydrin test kit (Kaiser test) purchased from Fluka Analytical was utilized to test for successful coupling or free

amines following deprotection steps. Avidin, egg white was purchased from EMD Biosciences, Inc.

Biotin Novatag Resin was purchased from Novabiochem Chemical Company (0.55 mmole/g loading) and TentaGel S RAM Fmoc Resin was purchased from Creo Salus Chemical Company (0.25mmol/g). 1'-Fmoc-amino-ferrocene carboxylic acid was purchased from Omm Scientific. All other reagents were purchased from commercial sources and used as received unless noted. Both **5** and **7** were air stable but stored at 4°C to avoid slow decomposition which was observed after several weeks.

**Physical Methods**

A Bruker Avance 400 MHz was utilized to obtain the NMR spectra in dimethyl sulfoxide-D6 (DMSO) as specified in the sections below. HR-MS was performed using the Agilent 6224 Accurate-Mass Time-Of-Flight (TOF) MS.

Cyclic voltammograms were acquired at room temperature using a BASi-C3 potentiostat equipped with a 3.0 mm glassy carbon working electrode, a platinum wire auxiliary electrode, and Ag/AgCl reference electrode. Measurements were performed under a blanket of nitrogen in 0.01 M phosphate buffer (pH = 7.4). The bioconjugates were dissolved in a stock solution of PBS buffer and allowed to stir overnight. Aliquots (10 mL) of these solutions were used to obtain cyclic voltammograms.

Fluorescent images were acquired using a Zeiss LSM-710 confocal microscope (Zeiss microscopy, Thornwood, NY). A 488 nm helium neon laser and a 543 nm argon laser were used to excite **7** and Cy3, respectively.

**Animals**

Male C57BL/6J mice (4–-6 month old), bred in the TCU vivarium from a breeding stock obtained from Jackson Laboratory (Bar Harbor, ME), were utilized in all experiments. All animals were housed and cared for in accordance with the Guide for the Care and Use of Laboratory Animals (National Research Council, 2010), and in accordance with protocols approved by the Institutional Animal Care and Use Committee (IACUC) of TCU. All subjects were housed in groups of three or four in standard cages (12.5 cm x 15 cm x 25 cm). All experimental groups and control groups were on the same light schedule, lights on at 0600 h and lights off at 1800 h. Both food and water were available *ad libitum*.

**Synthesis of 5: Biotin-Ferrocene-Cysteine Bioconjugate**

NovaTag Biotin resin (0.14 mmol, 250 mg) was allowed to swell in dimethylformamide (2 x 20 minutes) with shaking. Deprotection was achieved with 4-6 mL of 20% piperidine/dimethylformamide (2 x 20 minutes) with shaking. The resin was washed (3 x dimethylformamide, 3 x dimethylformamide:methanol, 3 x methanol:$CH_2Cl_2$, 3 x $CH_2Cl_2$). Deprotection was confirmed with the ninhydrin test (yellow = negative result, blue = free amine). The resin was then coupled to 1'-Fmoc-aminoferrocene carboxylic acid using a cocktail of 1'-Fmoc-aminoferrocene carboxylic acid (0.42 mmol, 203.3 mg), 1-hydroxybenzotriazole hydrate (0.42 mmol, 58.78 mg), diisopropyl carbodiimide (0.42 mmol, 0.06736 mL), diisopropyl ethyl

amine (0.42 mmol, 0.07577 mL), $CH_2Cl_2$ (~4 mL), and dimethylformamide (~1 mL), and 6 hours of shaking. The resin was then washed as described above. This was followed by removal of the Fmoc group with 4-6 mL of 20% piperidine/dimethylformamide (2 x 20 min) with shaking. After expelling the reaction mixture twice, the wash cycle was carried out. The ninhydrin test was used to verify deprotection of the resin-bound compound by the appearance of a blue color. The compound was then coupled to Fmoc-Cys(Trt)-OH using a cocktail of Fmoc-Cys(Trt)-OH (0.42 mmol, 254.8 mg), 1-hydroxybenzotriazole hydrate (0.42 mmol, 58.78 mg), diisopropyl carbodiimide (0.42 mmol, 0.06736 mL), diisopropyl ethyl amine (0.42 mmol, 0.07577 mL), $CH_2Cl_2$ (~4 mL), and dimethylformamide (~1 mL), and 6 hours of shaking. The resin was then washed as described above. This was followed by removal of the Fmoc group with 4-6 mL of 20% piperidine/dimethylformamide (2 x 20 min) with shaking. After expelling the reaction mixture twice, the wash cycle was carried out. The ninhydrin test was used to verify deprotection of the resin-bound compound by the appearance of a blue color. The compound was cleaved from the resin using a cleaving cocktail of trifluoroacetic acid (120 mmol, 9.45 mL), MilliQ $H_2O$ (14 mmol, 0.25 mL), 1,2-ethanedithiol (3.0 mmol, 0.25 mL), and triisopropyl silane (0.49 mmol, 0.10 mL), and 4 hours of shaking. The solution was decanted into an ependorff tube, and excess trifluoroacetic acid was blown off with air. **5** was precipitated via addition of cold ethyl ether to the solution. The mixture was centrifuged at 3000 rpm for 5 minutes, and the resulting supernatant was removed. This process of ethyl ether addition, centrifugation, and supernatant removal was repeated 3 times or until the

supernatant was clear. The solid was dried on a lyophilizer overnight to isolate **5** as a tan powder. Yield (based on resin loading): 69.7 mg (78.1%).$^{1}$H NMR (DMSO, 400 MHz) δ: 6.5 (d, 2H, biotin NH), 4.8 (s, 2H, residual water), 4.7 (d, 2H, biotin NH), 4.6 (s, 1H, ferrocene amino carboxylic acid NH), 4.5 (s, 1H, SH), 4.4 (d, 2H, $NH_2$), 4.33 (s, 1H, biotin CH or cysteine CH), 4.29 (m, 1H, biotin CH), 4.15 (s, 2H, biotin $CH_2$ or cysteine $CH_2$), 4.13 (m, 1H, biotin CH), 4.0 (s, 2H, biotin $CH_2$ or cysteine $CH_2$), 3.9 (s, 1H, biotin CH or cysteine CH), 3.4 (q, 4H, residual ethyl ether), 3.2-2.6 (m, 12H, biotin $CH_2$, ferrocene CH), 2.5 (s, 6H, DMSO), 2.1 (t, 2H, biotin $CH_2$), 1.5 (m, 4H, biotin $CH_2$), 1.3 (m, 2H, biotin $CH_2$), 1.0 (t, 6H, residual ethyl ether). MALDI-MS: m/z = 1231.4454 (30%, $[2M+H]^+$), 617.2490 (100%, $[M+H]^+$). Theoretical $[M+H]^+$: 617.16. Observed $[M+H]^+$: 617.2490.

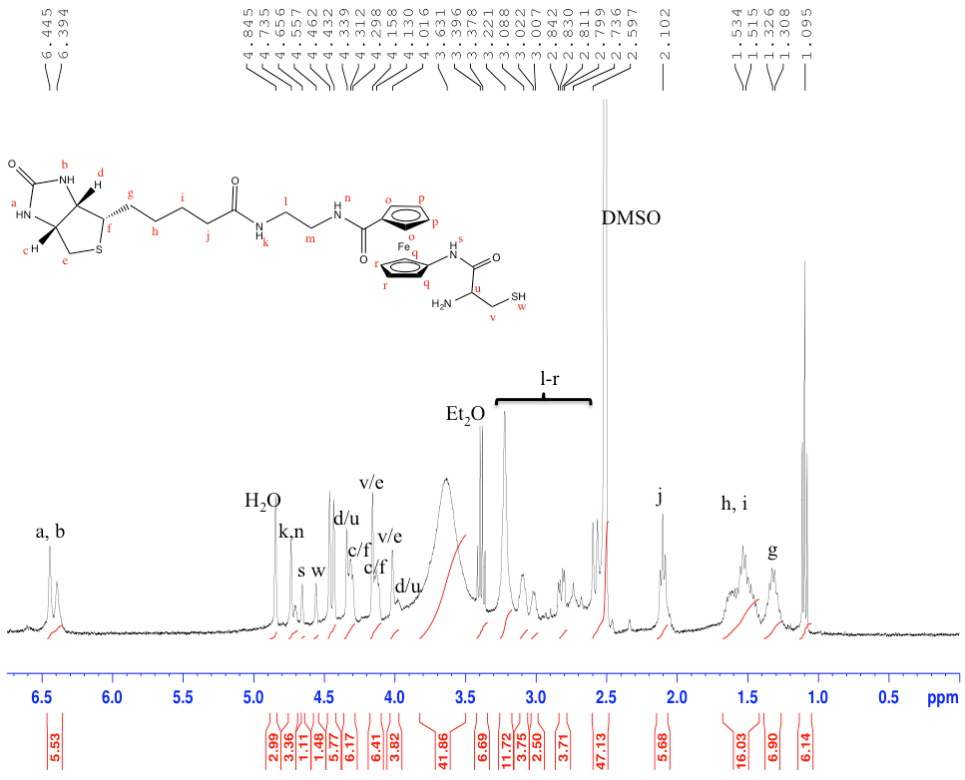


**Figure 5**: $^{1}$H NMR of **5** in DMSO with labeled molecular diagram.

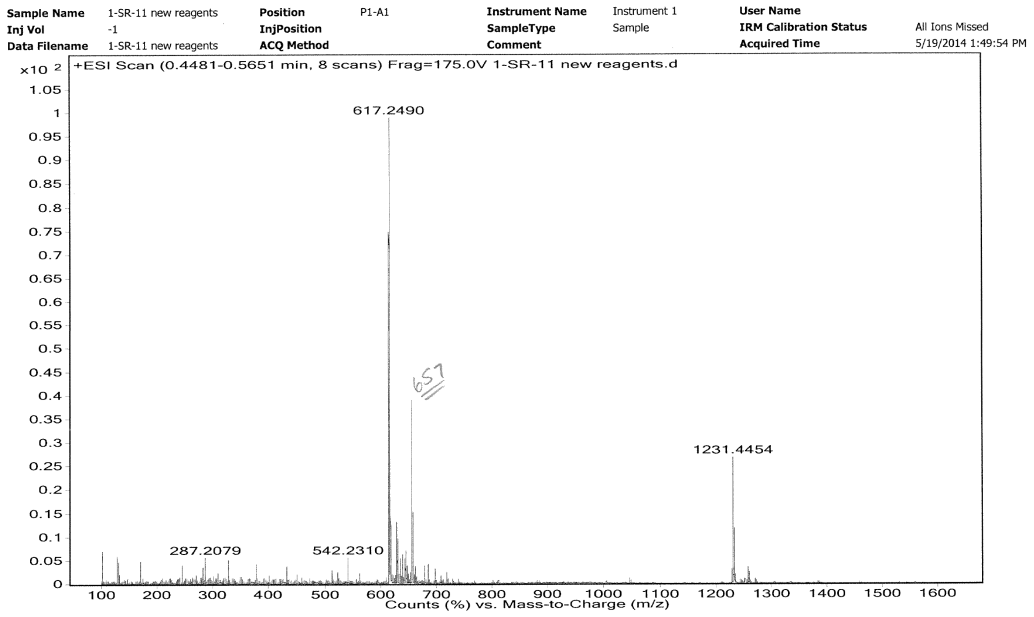


**Figure 6**: MALDI-MS of **5** in MeOH.

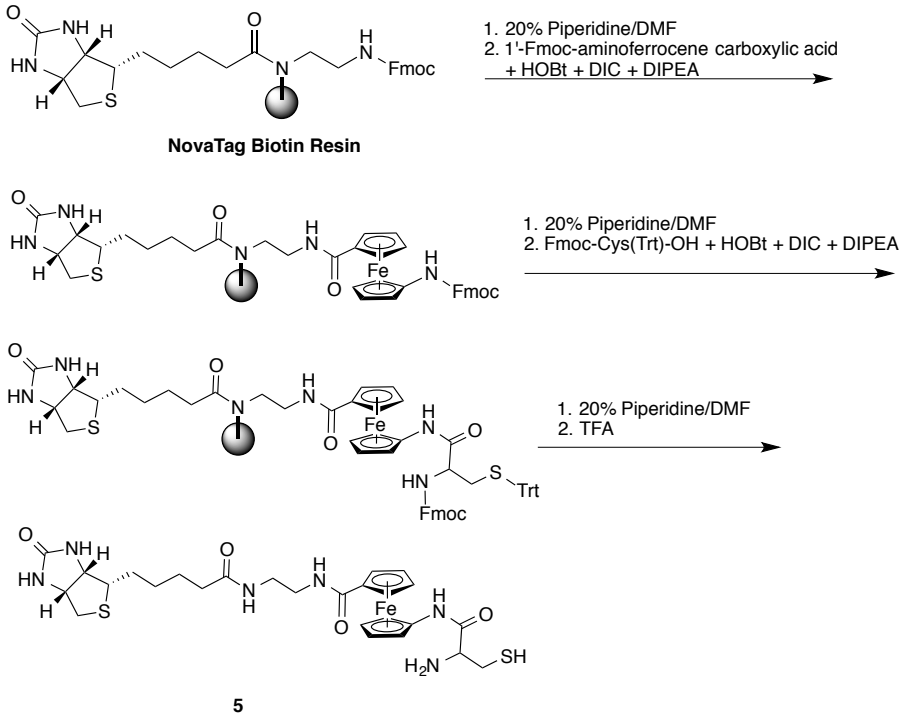


**Figure 7**: Synthetic methods used to produce **5**.

**Cyclic Voltammetry and Square Wave Analysis of 5**

Compound **5** (0.112 mmol, 68.78 mg) was added to 60 mL of 1 mM PBS and the solution was allowed to stir overnight. Five solutions comprised of **5** (8 mL) and varying concentrations of avidin from egg white (0, 1.9, 3.8, 7.5, 15 μM) were prepared and allowed to stir for 60 minutes. Cyclic voltammetry and square wave analysis (300 mV/s) were then performed on each solution, starting with the most dilute solution with respect to avidin and ending with the most concentrated. The glassy carbon working electrode was cleaned and polished between each measurement. Bovine serum albumin (4.80 μmol, 318.9 mg) was then added to each solution and allowed to stir for 30 minutes. Cyclic voltammetry and square wave analysis (300 mV/s) were performed on each, starting with the most dilute solution with respect to avidin and ending with the most concentrated. The glassy carbon working electrode was cleaned and polished between each measurement.

**Diffusion Studies of 5**

Compound **5** (0.0373 mmol, 22.92 mg) was added to 20 mL of 1mM PBS and the solution was allowed to stir overnight. A sample containing **5** (8 mL) and avidin from egg white (0.120 μmol, 7.92 mg) and a separate sample containing **5** (8 mL) and bovine serum albumin (4.80 μmol, 319 mg) were prepared and allowed to stir for 60 minutes. Cyclic voltammetry was then performed on each solution using a range of scan rates (ν). $\sqrt{\nu}$ was plotted against the $I_{pc}$ value derived from scan rate = 10 mV/s.

**Docking Studies with AutoDock Vina**

Docking studies of **5** were performed using previously determined models of avidin (PDB ID 1AVE) and albumin (PDB ID 3V03). The structure of **5** was optimized for the docking studies in ChemBio3D Pro 12.0 with the 646 MM2 energy minimization. AutoDock Tools was used to prepare the protein optimized structural files that were run with AutoDock Vina using PyRx to obtain the binding energies. The search space dimensions were selected in order to contain the entire peptide with an exhaustiveness of 650 runs. The visualization of the docking results were made using PyMol.

**Synthesis of 7: KLVFF-Fluorescein**

Rink resin (0.075 mmol, 300 mg) was allowed to swell in dimethylformamide (2 x 20 minutes) with shaking. Deprotection was achieved with 4-6 mL of 20% piperidine/dimethylformamide (2 x 20 minutes) with shaking. The resin was washed (3 x dimethylformamide, 3 x dimethylformamide:methanol, 3 x methanol:$CH_2Cl_2$, 3 x $CH_2Cl_2$). Deprotection was confirmed with the ninhydrin test (yellow = negative result, blue = free amine). The resin was then coupled to Fmoc-Phe-OH using a cocktail of Fmoc-Phe-OH (0.225 mmol, 87.17 mg), HBTU (0.225 mmol, 85.33 mg), diisopropyl carbodiimide (0.225 mmol, 0.0352 mL), diisopropyl ethyl amine (0.225 mmol, 0.0392 mL), $CH_2Cl_2$ (~4 mL), and dimethylformamide (~1 mL), and 6 hours of shaking. The resin was then washed as described above. This was followed by removal of the Fmoc group with 4-6 mL of 20% piperidine/dimethylformamide (2 x 20 min) with shaking. After expelling the

reaction mixture twice, the wash cycle was carried out. The ninhydrin test was used to verify deprotection of the resin-bound compound by the appearance of a blue color. The compound was then coupled to another Fmoc-Phe-OH using a cocktail of Fmoc-Phe-OH (0.225 mmol, 87.17 mg), HBTU (0.225 mmol, 85.33 mg), diisopropyl carbodiimide (0.225 mmol, 0.0352 mL), diisopropyl ethyl amine (0.225 mmol, 0.0392 mL), $CH_2Cl_2$ (~4 mL), and dimethylformamide (~1 mL), and 6 hours of shaking. The resin was then washed as described above. This was followed by removal of the Fmoc group with 4-6 mL of 20% piperidine/dimethylformamide (2 x 20 min) with shaking. After expelling the reaction mixture twice, the wash cycle was carried out. The ninhydrin test was used to verify deprotection of the resin-bound compound by the appearance of a blue color. The resin was then coupled to Fmoc-Val-OH using a cocktail of Fmoc-Val-OH (0.225 mmol, 76.36 mg), HBTU (0.225 mmol, 85.33 mg), diisopropyl carbodiimide (0.225 mmol, 0.0352 mL), diisopropyl ethyl amine (0.225 mmol, 0.0392 mL), $CH_2Cl_2$ (~4 mL), and dimethylformamide (~1 mL), and 6 hours of shaking. The resin was then washed as described above. This was followed by removal of the Fmoc group with 4-6 mL of 20% piperidine/dimethylformamide (2 x 20 min) with shaking. After expelling the reaction mixture twice, the wash cycle was carried out. The ninhydrin test was used to verify deprotection of the resin-bound compound by the appearance of a blue color. The resin was then coupled to Fmoc-Leu-OH using a cocktail of Fmoc-Leu-OH (0.225 mmol, 79.52 mg), HBTU (0.225 mmol, 85.33 mg), diisopropyl carbodiimide (0.225 mmol, 0.0352 mL), diisopropyl ethyl amine (0.225 mmol, 0.0392 mL), $CH_2Cl_2$ (~4 mL), and dimethylformamide (~1 mL), and 6 hours of shaking. The resin was

then washed as described above. This was followed by removal of the Fmoc group with 4-6 mL of 20% piperidine/dimethylformamide (2 x 20 min) with shaking. After expelling the reaction mixture twice, the wash cycle was carried out. The ninhydrin test was used to verify deprotection of the resin-bound compound by the appearance of a blue color. The resin was then coupled to Fmoc-Lys(Boc)-OH using a cocktail of Fmoc-Lys(Boc)-OH (0.225 mmol, 105.42 mg), HBTU (0.225mmol, 85.33mg), diisopropyl carbodiimide (0.225 mmol, 0.0352 mL), diisopropyl ethyl amine (0.225 mmol, 0.0392 mL), $CH_2Cl_2$ (~4 mL), and dimethylformamide (~1 mL), and 6 hours of shaking. The resin was then washed as described above. This was followed by removal of the Fmoc group with 4-6 mL of 20% piperidine/dimethylformamide (2 x 20 min) with shaking. After expelling the reaction mixture twice, the wash cycle was carried out. The ninhydrin test was used to verify deprotection of the resin-bound compound by the appearance of a blue color. The resin was then coupled to fluorescein isothiocyanate using a cocktail of fluorescein isothiocyanate (0.225 mmol, 76.36 mg), HBTU (0.225 mmol, 85.33 mg), diisopropyl carbodiimide (0.225 mmol, 0.0352 mL), diisopropyl ethyl amine (0.225 mmol, 0.0392 mL), $CH_2Cl_2$ (~4 mL), and dimethylformamide (~1 mL), and 6 hours of shaking. The resin was then washed as described above. This was followed by removal of the Fmoc group with 4-6 mL of 20% piperidine/dimethylformamide (2 x 20 min) with shaking. After expelling the reaction mixture twice, the wash cycle was carried out. The ninhydrin test was used to verify deprotection of the resin-bound compound by the appearance of a blue color. The compound was cleaved off the resin using a cleaving cocktail of trifluoroacetic acid (120 mmol, 9.45 mL), MilliQ

$H_2O$ (14 mmol, 0.25 mL), 1,2-ethanedithiol (3.0 mmol, 0.25 mL), and triisopropyl silane (0.49 mmol, 0.10 mL), and 4 hours of shaking. The solution was decanted into an ependorff tube, and excess trifluoroacetic acid was blown off with air. **7** was precipitated via addition of cold ethyl ether to the solution. The mixture was centrifuged at 3000 rpm for 5 minutes, and the resulting supernatant was removed. This process of ethyl ether addition, centrifugation, and supernatant removal was repeated 3 times or until the supernatant was clear. The solid was dried on a lyophilizer overnight to isolate **7** as an orange powder. Yield (based on resin loading): 61.5 mg (78.6%). MALDI-MS: m/z = 1047.8649 (5%, $[M+H]^+$), 524.4541 (100%, $[M/2+H]^+$), 377.3551 (20%, [fluorescein isothiocyanate + H]$^+$ Theoretical $[M+H]^+$: 1044.47. Observed $[M+H]^+$: 1047.8649.

.

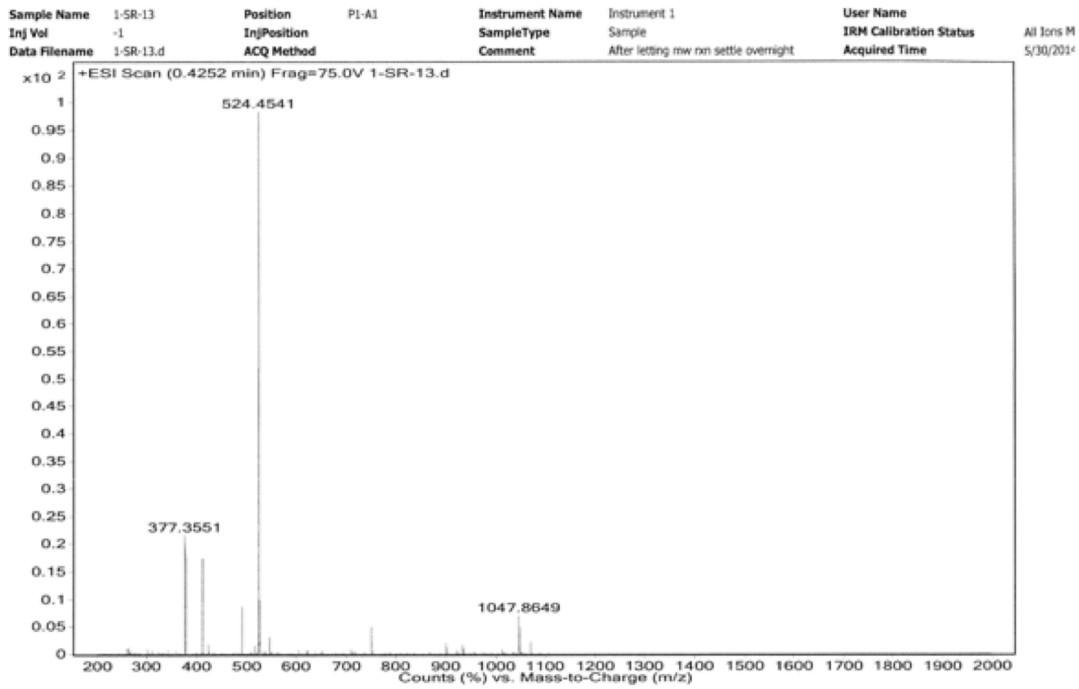


**Figure 8**: MALDI-MS of **7** in MeOH.

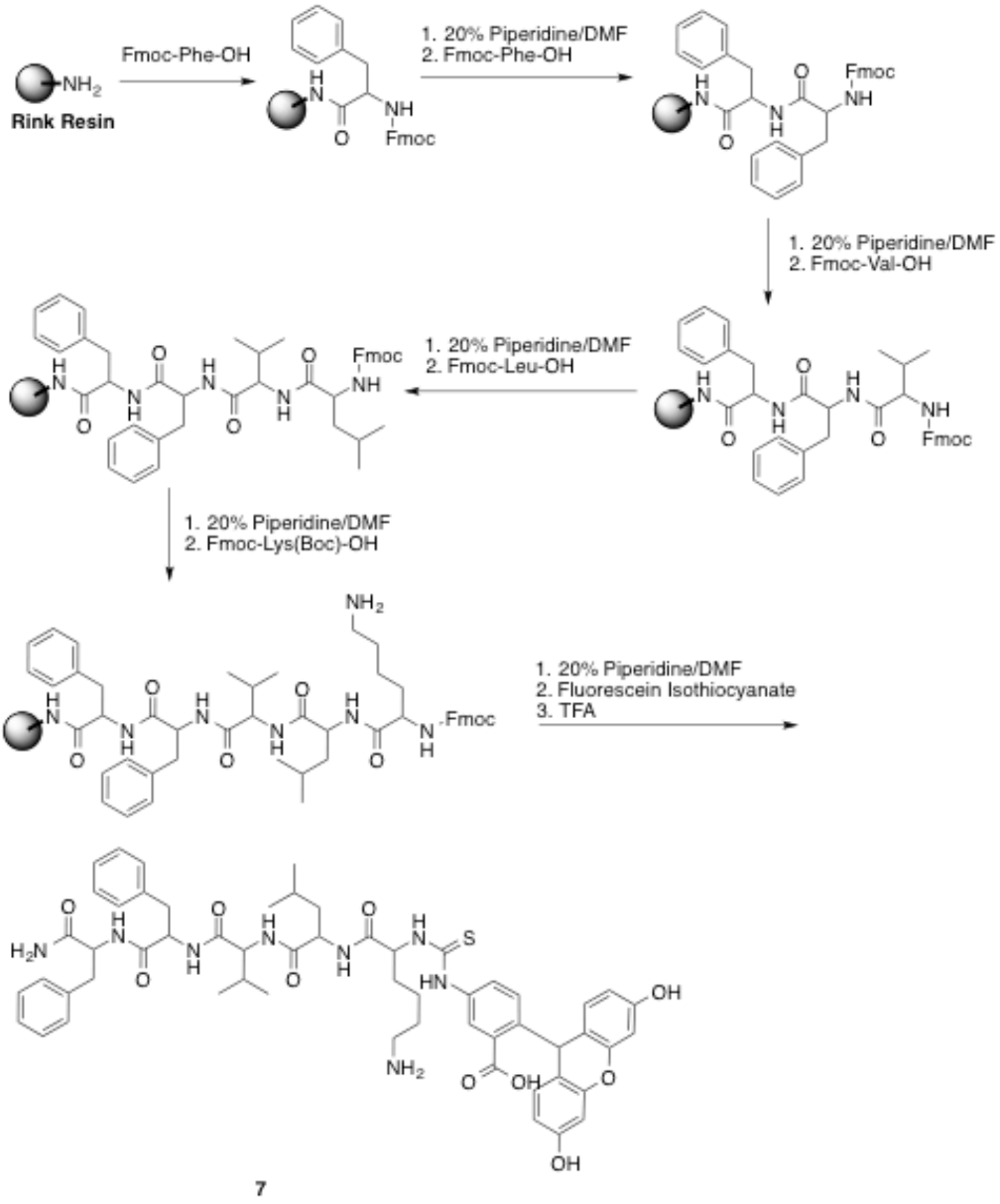


**Figure 9**: Synthetic methods used to produce **7**.

## Staining of C57BL/6 Cells with 7

C57BL/6 hippocampal tissue cultures were individually were blocked in phosphate buffered saline with Tween 20 (PBST) and 2% donkey serum on a well plate overnight. The blocking buffer was removed, and the tissues were washed with PBST (3 x 5 min) with shaking. The cells were exposed to mouse anti-Aβ

antibody 6E10 (Covance, Deadham, MA) at a 1:4000 dilution and shaken overnight at 40ºC. The supernatant was removed, and the tissues were washed with PBST (3 x 5 min) with shaking. The cells were then exposed to donkey anti-mouse IgG Cy3 antibody (Jackson ImmunoResearch, West Grove, PA) at a 1:1000 dilution and shaken for 2 hours at room temperature. The supernatant was removed, and the tissues were washed with PBST (3 x 5 min) with shaking. The cells were then exposed to a 1.0 mg/mL solution of **7** in methanol and shaken for 2 hours at room temperature. The supernatant was removed, and the tissues were washed with PBST (3 x 5 min) with shaking. Fluorescent images were taken on a Zeiss LSM-710 confocal microscope (Zeiss microscopy, Thornwood, NY). A 488 nm helium neon laser and a 543 nm argon laser were used to excite **7** and Cy3, respectively.

**Staining of C57BL/6 Cells with 7, Alternate Order of Addition**

C57BL/6 tissue cultures were individually were blocked in phosphate buffered saline with Tween 20 (PBST) and 2% donkey serum on a well plate overnight. The blocking buffer was removed, and the tissues were washed with PBST (3 x 5 min) with shaking. The cells were exposed to a 1.0 mg/mL solution of **7** in methanol and shaken for 2 hours at room temperature. The supernatant was removed, and the tissues were washed with PBST (3 x 5 min) with shaking. The cells were then exposed to mouse anti-Aβ antibody 6E10 (Covance, Deadham, MA) at a 1:4000 dilution and shaken overnight at 40ºC. The supernatant was removed, and the tissues were washed with PBST (3 x 5 min) with shaking. The cells were then exposed to donkey anti-mouse IgG Cy3 antibody (Jackson ImmunoResearch, West

Grove, PA) at a 1:1000 dilution and shaken for 2 hours at room temperature. The supernatant was removed, and the tissues were washed with PBST (3 x 5 min) with shaking. Fluorescent images were taken on a Zeiss LSM-710 confocal microscope (Zeiss microscopy, Thornwood, NY). A 488 nm helium neon laser and a 543 nm argon laser were used to excite **7** and Cy3, respectively.

# RESULTS AND DISCUSSION

## Project 1: Electrochemical Sensor Development Through Ferrocene-Biotin Bioconjugates

Prior studies on solutions containing only **5** and avidin revealed a strong, inversely proportional relationship between avidin concentration and peak current intensity over an avidin concentration range of 15-75 μM (*19*). While this trend was an exciting discovery, its utility was limited because the solutions used were too pure and the concentrations analyzed were too high to accurately represent the complex environments found within biological systems. As such, the following experiments were designed to give insight into how compound **5** would behave in solutions containing both impurities (bovine serum albumin) and lower concentrations of avidin (1.875-15 μM). As shown in Figure 10, square wave voltammetry was used to study the changes in current intensity of **5** with varying of concentrations of avidin in the presence of albumin (0.6 mM). Square wave voltammetry was chosen as the method of analysis because of its increased sensitivity compared to cyclic voltammetry. However, since the sweep width on a

given square wave voltammogram is significantly smaller than that of a given cyclic voltammogram, cyclic voltammetry was performed first to give insight into the parameters to be used in the square wave experiments and its results are shown in Figure 11.

**Square Wave Response of 5 to Avidin in the Presence of Albumin**

For this series of experiments, the albumin concentration was maintained at a concentration of 0.6 mM to parallel that found in human serum (*20*). Overall, a consistent drop in current was observed with increasing concentrations of avidin, consistent with what we showed in the experiments *sans* albumin. A plot of avidin concentration versus the area under each square wave resulted in a straight line ($R^2$ = 0.945), as shown in the insert in Figure 10. The linearity of this trend suggests that we can use this method to evaluate samples with unknown concentrations of avidin at low, micromolar concentrations in the presence of high concentrations of albumin.

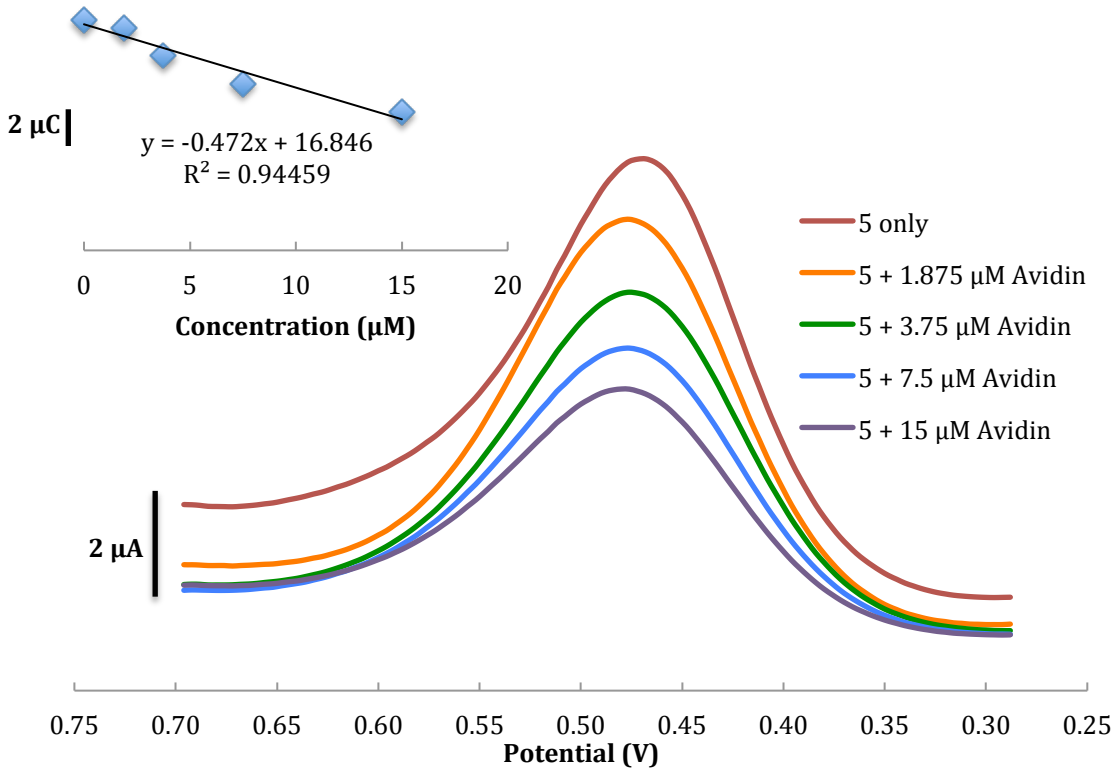


**Figure 10**: SW overlay of the $Fe^{III}/Fe^{II}$ couple of **5** (1.9 mM) + albumin (0.6 mM) + avidin at various concentrations using PBS Buffer (pH=7.4) as a solvent, a scan rate of 300 mV/s, an Ag/AgCl reference electrode, and a glassy-carbon working electrode. The inset shows the linear correlation of the current response to avidin.

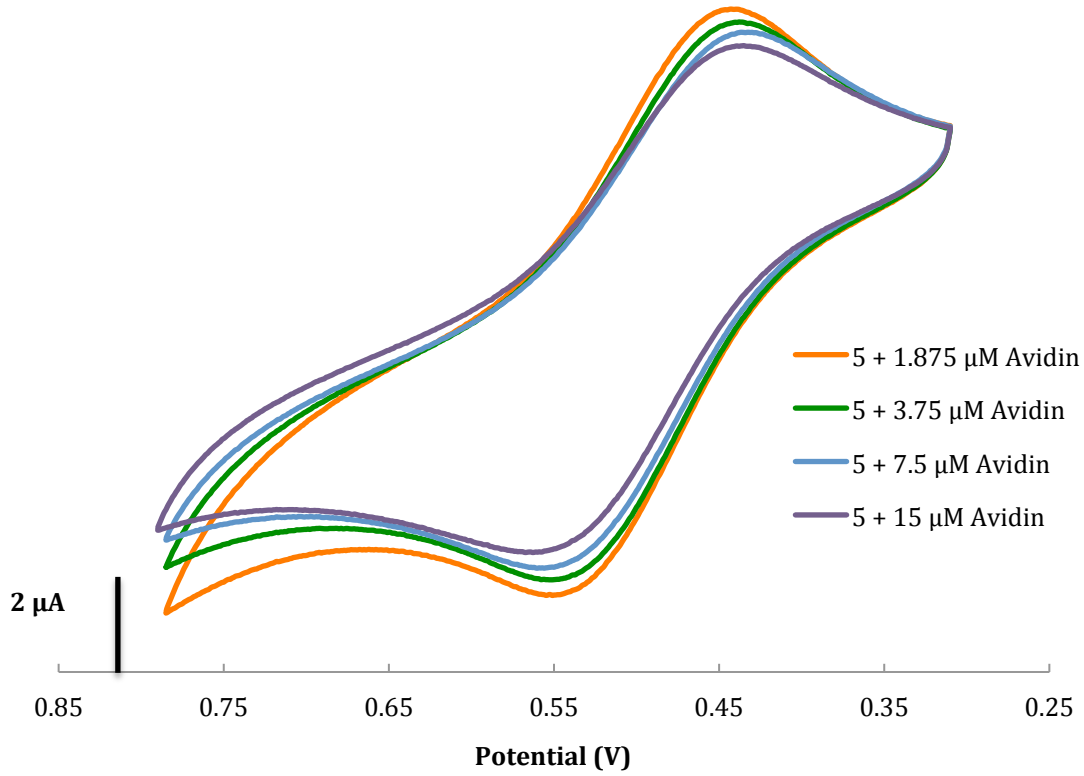


**Figure 11**: CV overlay of the $Fe^{III}/Fe^{II}$ couple of **5** (1.9 mM) + albumin (0.6 mM) + avidin at various concentrations using PBS Buffer (pH=7.4) as a solvent, a scan rate of 300 mV/s, an Ag/AgCl reference electrode, and a glassy-carbon working electrode.

## Diffusion Studies

We next set out to determine whether or not the working electrode used to collect the electrochemical data from the previous experiment was a result of diffusion of the analyte molecules or other mechanisms such as analyte decomposition or deposition on the electrode surface. Scans over a range of scan rates (ν) for solutions containing **5** and either avidin or albumin were collected. The $\sqrt{\nu}$ was plotted against the $I_{pc}$ value derived from ν = 10 mV/s, and the results are shown in Figures 12 and 13. The linearity of each plot was consistent with a diffusion-controlled electron transfer process as opposed to interference from the working electrode surface and species in solution (*38*).

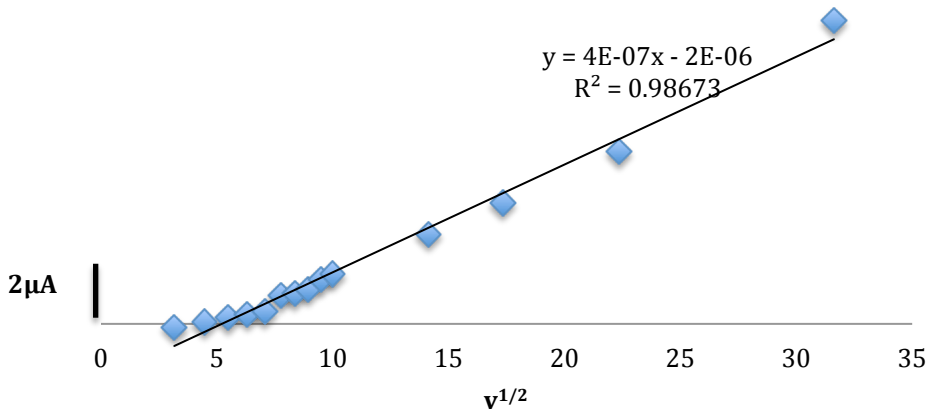


**Figure 12**: Plot of the $\sqrt{\nu}$ vs. $I_{pc}$ value from a cyclic voltammogram of **5** + 0.6 mM avidin at that scan rate using PBS Buffer (pH=7.4) as a solvent, an Ag/AgCl reference electrode, and a glassy-carbon working electrode.

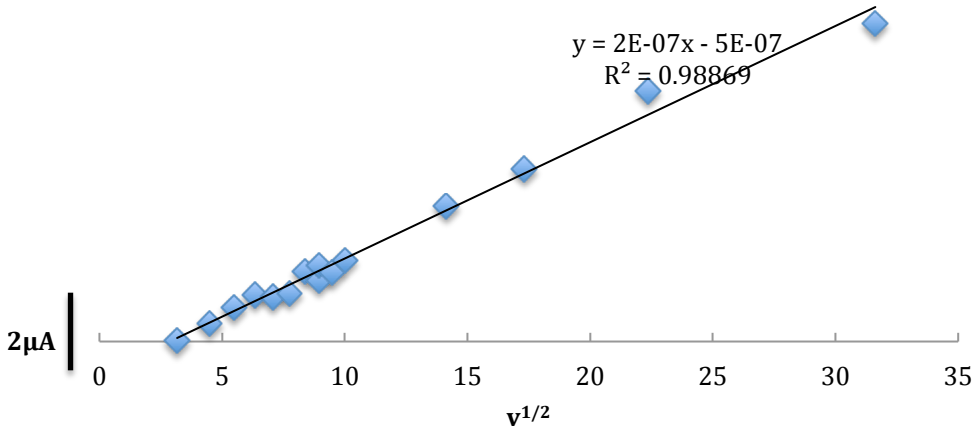


**Figure 13**: Plot of the $\sqrt{\nu}$ vs. the $I_{pc}$ value from a cyclic voltammogram of **5** + 0.6 mM avidin at that scan rate using PBS Buffer (pH=7.4) as a solvent, an Ag/AgCl reference electrode, and a glassy-carbon working electrode.

**Docking Studies with Autodock Vina**

While the results of the square wave and diffusion studies were promising, we sought to acquire more supporting data for our bioconjugate model. Autodock Vina was used to visually model the theoretical interactions between **5** and either avidin or albumin and calculate the strength of these theoretical interactions through an energetic lens. As shown in Figure 14, the biotin component of **5** interacts with the β-barrel binding site of avidin as expected (*39-41*). In these models, the biotin moiety is indeed the targeting component responsible for the interaction as evidenced by the biotin being buried in the barrel in the lowers energy conformations. The ferrocene moiety, in contrast, twists slightly in each model and projects out of the avidin. This suggests that the avidin binding interaction is largely unaffected by the presence of the ferrocene moiety. The well-defined interactions modeled here are in stark contrast to the random, electrostatic interactions observed between **5** and albumin in Figure 15. The observations noted in the visual models are quantified in the molar affinity values shown in Table 1. With prevalent intermolecular forces such as dipole-dipole interactions having dissociation energies as low as 2 kJ/mol (*42*), the difference of 0.5 kcal/mol (2.092 kJ/mol) between the two sets of interactions suggests that **5** has a significantly higher affinity with avidin than with albumin. In addition, the similarity between the energies of the five most stable conformations between **5** and albumin suggests that the interaction between the two compounds is random and non-specific.

| Mode | Affinity (kcal/mol) | |
|---|---|---|
| | **5** + Albumin | **5** + Avidin |
| 1 | -8.4 | -8.9 |
| 2 | -8.4 | -8.8 |
| 3 | -8.4 | -8.6 |
| 4 | -8.4 | -8.6 |
| 5 | -8.3 | -8.5 |

**Table 1**: Molar affinity data for **5** + albumin and **5** + avidin as provided by Autodock Vina using an exhaustiveness of 650 runs.

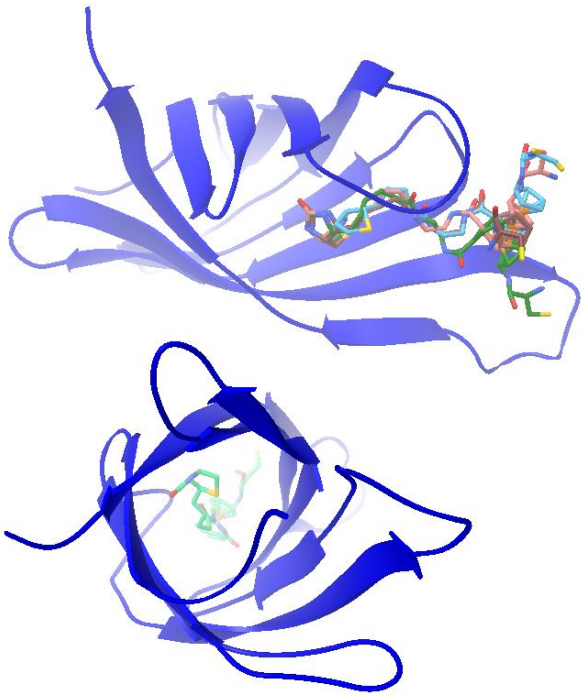

**Figure 14**: Visualization of docking results for **5** + avidin (PDB 1AVE) performed with an exhaustiveness of 650 runs.

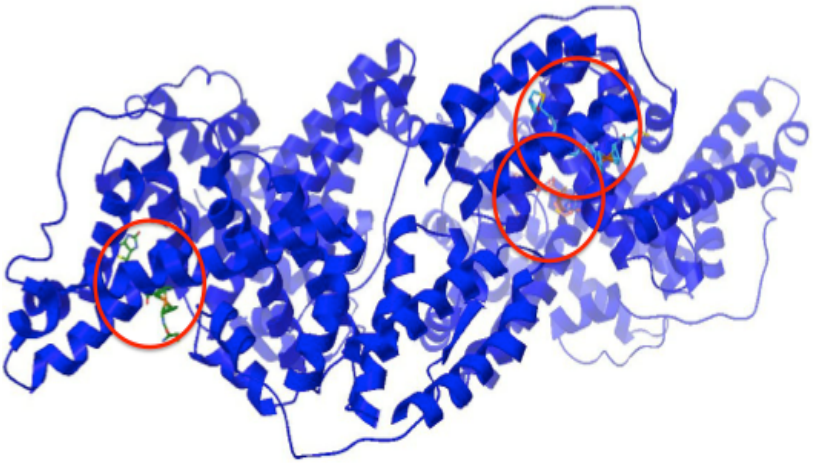

**Figure 15**: Visualization of docking results for **5** + albumin (PDB 3V03) performed with an exhaustiveness of 650 runs.

## Project 2: Development of Biosensor Technology for Amyloid Protein

My second project focused on the application of the bioconjugate model studied in my first project to the amyloid-β (Aβ) protein aggregates associated with Alzheimer's Disease. If avidin concentrations could be measured using ferrocene-biotin bioconjugates, it is possible that Aβ concentrations could be measured in solution using ferrocene bioconjugates designed to be sensitive for Aβ proteins and electrochemical techniques similar to those performed in the previous studies. However, before such experiments could be formed, it would be important to verify that the molecular-binding component of the proposed bioconjugate, KLVFF, could reliably and specifically interact with Aβ plaques. To verify the specificity of KLVFF for Aβ, fluorescently-labeled KLVFF molecules were exposed to C57BL/6 tissue samples rich in Aβ monomers and plaques. C57BL/6 mice are genetically engineered to produce Aβ monomers from birth, and Aβ plaques have been found to aggregate in the hippocampus within as few as 2 months of life (*35*). Since the brain

tissues studied were harvested from 6 month old mice, ample plaques were present and available for treatment with **7**.

**Tissue Stains with 7**

In the first experiment, the hippocampal tissue cultures were treated with the 1º and 2º antibody before the solution of **7**. This is significant because the 1º antibody and peptide moiety of **7** have been shown to interact with Aβ at similar binding sites (*27-34, 43*), and it is possible that the two compounds could serve as competitors for these binding sites. This competition hypothesis is supported by the results shown in Figure 16. Compound **7** was shown interacting with the cells around the plaques, as represented by the green fluorescence around the plaques. This is possibly due to the molecules of **7** interacting with Aβ monomers present in the surrounding cells but unlabeled by the larger, bulkier antibodies used to stain the plaques. It is also possible that **7** is simply able to interact with surface proteins and/or other extracellular components present on the exposed cells, thus making the entire tissue culture appear to be covered in **7**. Regardless of the reason, this would not be a problem if it appeared that **7** also interacted with the Aβ plaques, as that was the primary goal of the stain experiments. However, this does not appear to be the case, as the solid red color of the plaques suggests that they are bound by antibodies and antibodies alone; the plaques would appear to be a mix of both red and green if they were bound significantly by both **7** and the antibodies. The absence of green on the plaques supports the competition hypothesis mentioned earlier and also inspired the design of the second experiment.

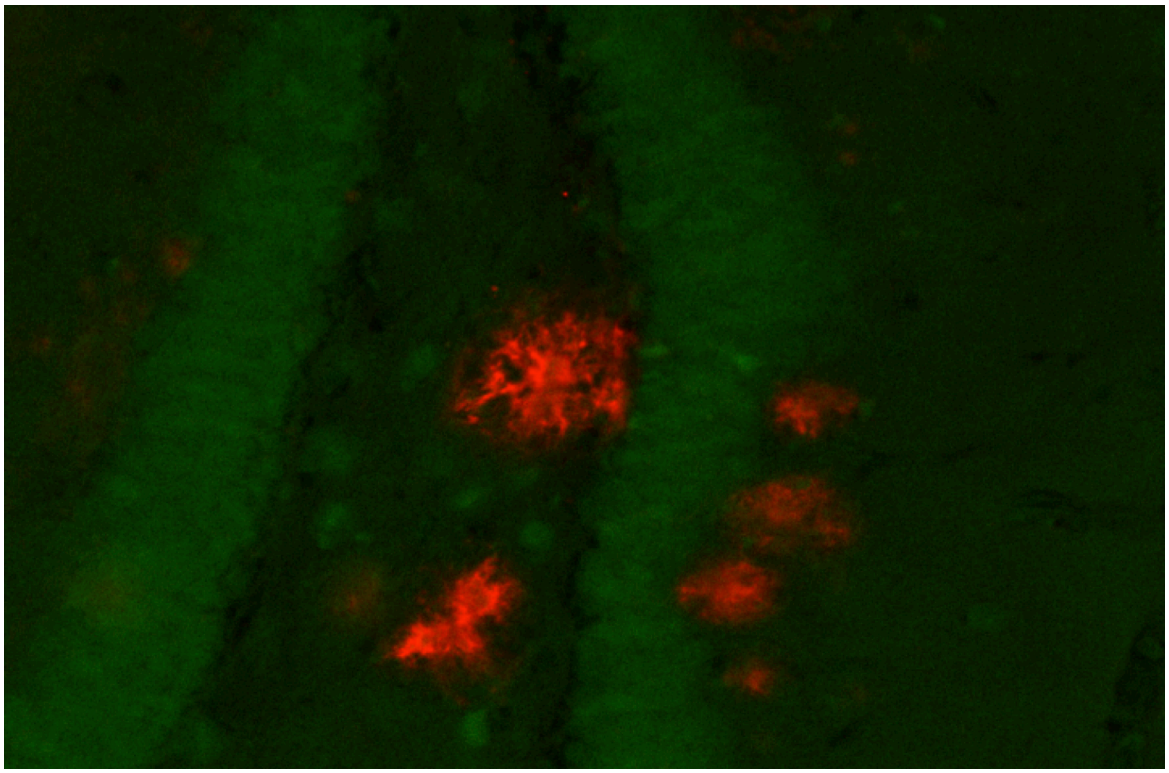

**Figure 16**: LSM image overlay of C57BL/6 cell tissue treated with 1º and 2º antibody, followed by **7**. Green fluorescence represents **7**, and red fluorescence represents antibody-labeled Aβ plaques.

In the second experiment, the brain tissues were exposed to **7** before the 1º antibody. This was done to determine if **7** would be able to interact with the Aβ peptide to a greater extent than in the previous experiment. Unfortunately, the uniform red staining of the plaques suggests that little to no **7** was bound to the plaques. This color uniformity is reinforced when comparing the shades of red in the view showing the tissue and antibodies (top right) and the two-view overlay (bottom left). If the antibody-bound Aβ plaques also had **7** bound to them, the plaques in the overlay would appear to be a mix of red and green, and when comparing those two images it is clear that there was no **7** bound to the Aβ plaques.

This may still be due to competition for the same binding site, but if the 1º antibody has higher affinity for the site than the peptide moiety on **7** does then the antibody may be able to occupy the spot regardless of order of addition. It may also be due to how physically compact the monomers are within the plaques. Even if the antibody has a higher affinity for the binding sites compared to compound **7**, the smaller molecular size of **7** may allow it to penetrate the plaque deeper than the antibodies and thus could possibly bind to binding sites buried on the inside while the antibodies occupy those on the outside. However, if the plaques were too tightly aggregated for **7** to penetrate, only the binding sites exposed on the outside would be available for either of the two reagents to interact with. Future studies could utilize different antibodies and/or different peptide moieties to further explore the interaction between a potential peptide moiety and its interaction with Aβ plaques.

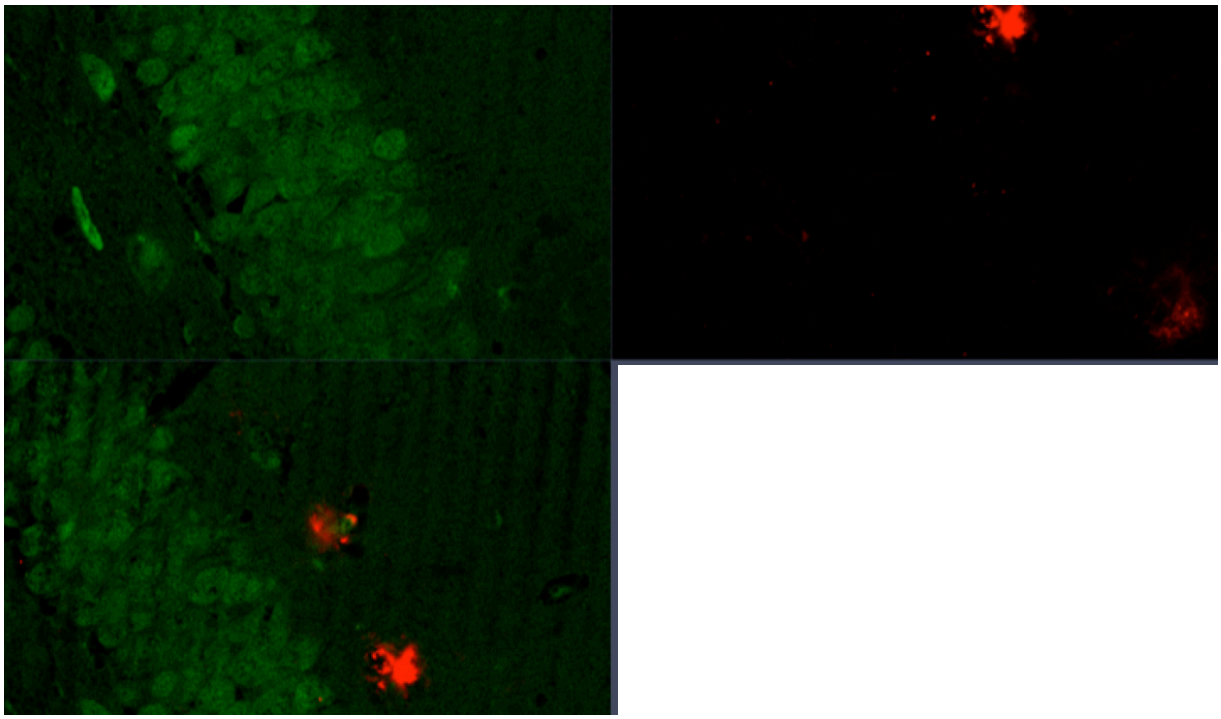

**Figure 17**: Side-by-side LSM images of C57BL/6 cell tissue treated with **7**, followed by 1º and 2º antibody. Green fluorescence represents **7**, and red fluorescence represents antibody-labeled Aβ plaques. Top left: tissue + **7** only. Top right: tissue + antibodies only. Bottom left: overlay of the top two images.

# CONCLUSION

## Project 1:

Building off of the prior work Scarborough et al. prior work, a ferrocene-biotin bioconjugate (**5**) was electrochemically evaluated in dilute and impure solutions using cyclic and square wave voltammetry experiments. These studies showed that the strong, inversely proportional relationship between avidin concentration and peak current originally observed by Scarborough et al. holds true even as avidin concentrations are brought as low as 1.875 μM and reactive impurities such as albumin are added to the evaluated solutions. Overall, these

results suggest the bioconjugate model utilized in **5** is viable and could potentially be adjusted for clinical use by replacing the biotin moiety with one specific for a pathogen or other compound of interest.

## Project 2:

This project explored the possibility of replacing that moiety with KLVFF, a peptide shown to be specific for Aβ, a compound whose aggregates are frequently associated with Alzheimer's Disease. Before electrochemical experiments could be performed as in the avidin studies, tissue stains were performed in an effort to verify the specificity of KLVFF for Aβ. While two separate stains were performed on C57BL/6 hippocampal tissues, we were unable to successfully establish a specific interaction between KLVFF and Aβ. Overall, the avidin studies provided strong support for the bioconjugate model utilized in **5** and laid the groundwork for its extension into clinical application, which began in the peptide studies. Further research into the KLVFF-Aβ interaction may help provide the insight necessary to determine whether a KLVFF-ferrocene bioconjugate could be used to measure Aβ concentration in solution or if the peptide moiety used in our studies needs to be adjusted to achieve higher levels of specificity.

# REFERENCES


1. Hsieh, K.; Ferguson, B. S.; Eisenstein, M.; Plaxco, K. W.; Soh, H. T. Integrated Electrochemical Microsystems for Genetic Detection of Pathogens at the Point of Care. *Acc. Chem. Res.* **2015**, ASAP.
2. Wang, J. Electrochemical Biosensors: Towards Point-of-Care Cancer Diagnosis. *Biosens. Bioelectron.,* **2006**, *21*: 1887-1892.
3. Zhang, S.; Zheng, F.; Wu, Z.; Shen, G.; Yu, R. Highly Sensitive Electrochemical Ddetection of Immunospecies Based on Combination of Fc Label and PPD Film/Gold Nanoparticle Amplification. *Biosens. Bioelectron.,* **2008**, *24*: 129-135.
4. Meares, C. Editorial: Introduction to Bioconjugate Chemistry. *Bioconjugate Chem.* **2013**, *24* (1): 1-3.
5. Borisov, S. M.; Wolfbeis, O. S. Optical Biosensors. *Chem. Rev.*, **2008**, *108* (2): 423-461.
6. Fromwell, K.; Hulting, G.; Ilichev, A.; Larsson, A.; Caldwell. K. D. Particulate Platform for Bioluminescent Immunosensing. *Anal. Chem.,* **2007**, *79* (22): 8601-8607.
7. Tamura, T.; Hamachi, I. Recent Progress in Design of Protein-Based Fluorescent Biosensors and Their Cellular Applications. *ACS Chem. Biol*. **2014**, *9* (12): 2708-2717.
8. Toma, M.; Jonas, U.; Mateescu, A.; Knoll, W.; Dostalek, J. Active Control of SPR by Thermoresponsive Hydrogels for Biosensor Applications. *J. Phys. Chem.*, **2013**, *117* (22): 11705-11712.
9. Szarka, Z.; Kuik, Á.; Skoda-Földes, R.; Kollár, L. Aminocarbonylation of 1,1′-diiodoferrocene, two-step synthesis of heterodisubstituted ferrocene derivatives via homogeneous catalytic carbonylation/coupling reactions. *J. Organomet. Chem.,* **2004,** *689*: 2770-2775.
10. Niu, H. T.; Yin, Z.; Su, D.; Niu, D.; He, J.; Cheng, J. P. Imidazolium-based macrocycles as multisignaling chemosensors for anions. *Dalton Trans*., **2008**: 3694-3700.
11. Qing, G.-Y.; Sun, T.-L.; Wang, F.; He, Y.-B.; Yang, X. Chromogenic Chemosensors for N-Acetylaspartate Based on Chiral Ferrocene-Bearing Thiourea Derivatives. *European J. of Org. Chem.*, **2009**: 841-849.
12. Romero, T.; Caballero, A.; Espinosa, A.; Tarraga, A.; Molina, P. A multiresponsive two-arm ferrocene-based chemosensor molecule for selective detection of mercury, *Dalton Trans*., **2009**: 2121-2129.
13. Zapata, F.; Caballero, A.; Espinosa, A.; Tarraga, A.; Molina, P. A selective redox and chromogenic probe for Hg(II) in aqueous environment based on a ferrocene-azaquinoxaline dyad. *Inorg. Chem.,* **2009**: *48*: 11566-11575.
14. Alfonso, M.; Tarraga, A.; Molina, P. Ferrocene-based multichannel molecular chemosensors with high selectivity and sensitivity for Pb(II) and Hg(II) metal cations. *Dalton Trans.,* **2009**, *39*: 8637-8645.

15. Zapata, F.; Caballero, A.; Molina, P.; Tarraga, A. A ferrocene-quinoxaline derivative as a highly selective probe for colorimetric and redox sensing of toxic mercury(II) cations. *Sensors (Basel),* **2010**, *10*: 11311-11321.
16. Thakur, A.; Sardar, S.; Ghosh, S. A highly selective redox, chromogenic, and fluorescent chemosensor for Hg2+ in aqueous solution based on ferrocene-glycine bioconjugates. *Inorg. Chem.* **2011**, *50*: 7066-7073.
17. Dai, L.; Tu, T.; You, S.; Deng, W.; Hou, X. Asymmetric Catalysis with Chiral Ferrocene Ligands. *Acc. Chem. Res.* **2003**, *36* (9): 659-667.
18. Góngora-Benítez, M.; Tulla-Puche, J.; Albericio, F. Handles for Fmoc Solid-Phase Synthesis of Protected Peptides. *ACS Comb. Sci.* **2013**, *15* (5): 217-228.
19. Scarborough, J. H.; Brusoski, K.; Brewer, S.; Rodich, S.; Chatley, K. S.; Nguyen, T.; Green, K. N. Development of Low Molecular Weight Ferrocene-Biotin Bioconjugates as Electrochemical Sensors. *Organometallics*., **2015**, *34* (5): 918-925.
20. Harmonization of Reference Intervals. *Pathology Harmony*. **2014**.
21. Peters, Theodore. *All About Albumin: Biochemistry, Genetics, and Medical Applications*. Academic Press: California, pp 234; 285-316.
22. Cynis, H.; Scheel, E.; Saido, T. C.; Schilling, S.; Demuth, H. Amyloidogenic Processing of Amyloid Precursor Protein: Evidence of a Pivotal Role of Glutaminyl Cyclase in Generation of Pyrogultamate-Modified Amyloid-β. *Biochemistry*, **2008**, *47* (28): 7405-7413.
23. Sayre, L. M.; Perry, G.; Smith, M. A. Oxidative Stress and Neurotoxicity. *Chem. Res. Toxicol*. **2008**, *21* (1): 172-188.
24. Ridgley, D. M.; Barone, J. R. Evolution of the Amyloid Fiber over Multiple Length Scales. *ACS Nano.* **2013**, *7* (2): 1006-1015.
25. Lemkul, J. A.; Bevan, D. R. The Role of Molecular Simulations in the Development of Inhibitors of Amyloid β-Peptide Aggregation for the Treatment of Alzheimer's Disease. *ACS Chem. Neurosci*. **2013**, *3* (11): 845-856.
26. Portelius, E.; Westman-Brinkmalm, A.; Zetterberg, H.; Blennow, K. Determination of β-Amyloid Signatures in Cerebrospinal Fluid Using Immunoprecipitation-Mass Spectrometry. *J. Proteome Res.* **2006**, *5* (4): 1010-1016.
27. Castelletto, V.; Newby, G. E.; Hamley, I. W. Interactions of KLVFF-PEG Peptide Conjugate with Fibrinogen in Neutral Aqueous Solutions. *Macromol. Biosci*., **2008**, *8*: 1182-1189.
28. Chafekar, S. M.; Malda, H.; Merkx, M.; Meijer, E. W.; Viertl, D.; Lashuel, H. A.; Baas, F.; Scheper, W. Branched KLVFF Tetramers Strongly Potentiate Inhibition of Beta-Amyloid Aggregation. *Chembiochem.,* **2008**, *8*: 1857-1864.
29. Lowe, T. L.; Strzelec, A.; Kiessling, L. L.; Murphy, R. M. Structure-Function Relationships for Inhibitors of Beta-Amyloid Toxicity Containing the Recognition Sequence KLVFF. *Biochemistry-Us*. **2001**, *40*: 7882-7889.
30. Moss, M. A.; Nichols, M. R.; Reed, D. K.; Hoh, J. H.; Rosenberry, T. L. The Peptide KLVFF-K-6 Promotes Beta-Amyloid(1-40) Protofibril Growth by Association but Does Not Alter Protofibril Effects on Cellular Reduction of 3-(4,5-dimethylthiazol-2-yl)-2,5-diphenyltetrazolium bromide (MTT). *Mol. Pharmacol.* **2003**, *64*: 1160-1168.

31. Richman, M.; Willick, S.; Skirtenko, N.; Gedanken, A.; Rahimipour, S. Proteinous Microspheres Containing Klvff Peptides Strongly Inhibit Amyloid-Beta Aggregation and Toxicity. *Biopolymers,* **2009**, *92*: 324-324.
32. Rzepecki, P.; Schrader, T. Beta-Sheet Ligands in Action: KLVFF Recognition by Aminopyrazole Hybrid Receptors in Water. *J. Am. Chem. Soc.,* **2005**, *127*: 3016-3025.
33. Watanabe, K.; Nakamura, K.; Akikusa, S.; Okada, T.; Kodaka, M.; Konakahara, T.; Okuno, H. Inhibitors of Fibril Formation and Cytotoxicity of Beta-Amyloid Peptide Composed of KLVFF Recognition Element and Flexible Hydrophilic Disrupting Element, *Biochem. Bioph. Res. Co*. **2002**, *290*: 121-124.
34. Wei, C. W.; Peng, Y.; Zhang, L.; Huang, Q. Y.; Cheng, M.; Liu, Y. N.; Li, J. Synthesis and Evaluation of Ferrocenoyl Pentapeptide (Fc-KLVFF) as an Inhibitor of Alzheimer's A Beta(1-42) Fibril Formation in vitro. *Bioorg. Med. Chem. Lett.* **2011**, *21*: 5818-5821.
35. Oakley, H.; Cole, S. L.; Logan, S.; Maus, E.; Shao, P.; Craft, J.; Guillozet-Bongaarts, A.; Ohno, M.; Disterhoft, J.; Van Eldik, L.; Berry, R.; Vassar, R. Intraneuronal beta-amyloid aggregates, neurodegeneration, and neuron loss in transgenic mice with five familial Alzheimer's disease mutations: potential factors in amyloid plaque formation. *J. Neurosci.,* **2006**. *26*(40):10129-10140.
36. Cy3 AffiniPure Donkey Anti-Mouse IgG (H+L). https://www.jacksonimmuno.com/catalog/products/715-165-150 (accessed March 27, 2015).
37. Fluorescein, FITC/DATF Technical Information. https://www.jacksonimmuno.com/technical/products/conjugate-selection/fitc (accessed March 27, 2015).
38. Bard, A. J.; Faulkner, L. R. *Electrochemical Methods Fundamentals and Applications*; 2nd ed.; John Wiley & Sons: 111 River Street, Hoboken, NJ 07030, 2001.
39. General, I. J.; Dragomirova, R.; Meirovitch, H. Absolute Free Energy of Binding of Avidin/Biotin, Revisited. *J. Phys. Chem.* **2012**
40. Hansen, D. E.; Tang, D.; Sanborn, J. A.; Marshall, M. D. (Strept)Avidin-Biotin: Two Interrelated Experiments for the Introductory Chemistry Laboratory. *J. Chem. Educ.,* **2006**, *83* (5): 777.
41. Paton, W. F.; Liu, F.; Paul, I. C. Avidin-Biotin Interaction. Crystal and Molecular Structures of Two Linked Models. *J. Am. Chem.,* **1979**, *101* (4): 1005-1013.
42. McCord P. Types of Interactions. http://ch301.cm.utexas.edu/section2.php?target=imfs/forces/typesofimfs.html (accessed March 23, 2015).
43. Beta Amyloid, 1-16 (6E10) Monoclonal Antibody, Purified Exclusively Provided by BioLegend. https://antibody.biolegend.com/pdfdatasheet.php?catalogno=SIG-39320 (accessed March 27, 2015).